# Analysis by Proton NMR of Changes in Liquid-Phase and Solid-Phase Components during Ripening of Banana

Qing Xiao Ni and Thomas M. Eads*

Department of Food Science and Whistler Center for Carbohydrate Research, 1160 Smith Hall, Purdue University, West Lafayette, Indiana 47906-1160

Changes in both solid-phase and liquid-phase components were observed by proton ($^1$H) nuclear magnetic resonance (NMR) on intact samples of edible banana tissue (pulp) during ripening. Solid-selective cross-relaxation NMR showed that rigid components dominated by starch decreased from 20% of fresh weight in the mature green stage to 2.0% in the ripe yellow stage. Transverse relaxation measurements and wide-line NMR verified that starch in banana is as rigid as in isolated hydrated granules from banana. A less rigid component was also detected. On the same samples, liquid-phase components were measured by low-speed magic angle spinning NMR. Resonances of water, sucrose, fructose, glucose, fatty acyl chains of mobile lipids, and organic acids were easily detected. During ripening, sucrose concentration changed from 2.2 to 8.5% fresh weight, fructose from 0.5 to 5.3%, and glucose from 0.4 to 4.3%. Also, conversion of starch to sugars was quantified. NMR analysis was conducted without tissue disruption, separations, chemical treatment, or other spectrometry. The potential applications of NMR for fruit and fruit product quality assessment and processing applications are discussed.

## INTRODUCTION

The methods of nuclear magnetic resonance afford the opportunity to quantify components of agricultural materials, including whole fruits and vegetables or samples of their intact tissues (Coombe and Jones, 1983; Wang and Wang, 1988, 1989; Chen et al., 1989; Ishida et al., 1989; Cho et al., 1991; Bellon et al., 1992; Ni and Eads, 1992, 1993). By selective observation of liquid-phase components, it was previously shown that the several sugars present in ripe fruit could be identified and quantified by low-speed magic angle spinning (MAS) carbon-13 ($^{13}$C) NMR (Ni and Eads, 1992) and that additional components present at much lower levels (~0.01%) can be detected and quantified by MAS proton ($^1$H) NMR (Ni and Eads, 1993).

Solid-like macromolecular structures can also be detected by NMR. These are important in governing texture (as in cell wall components) or for storing energy (as in starch granules). Solid components were not detected in our previous experiments with fruit, since nuclear magnetic interactions in solid phases cause line broadening in excess of the spectral window used in liquids detection. Conventional solids techniques, such as wide-line Fourier transform $^1$H NMR, can, in principle, detect the broad solid resonance (Eads, 1991; Wu et al., 1992), but in the case of high water content samples such as fruit, the liquid is in such great excess that it swamps the solid resonance. Alternatives might be to perform high-resolution solid-selective experiments such as combined rotation and magic angle spinning (CRAMPS) for $^1$H observation or cross-polarization, magic angle spinning, high-power proton decoupling for $^{13}$C observation (Baianu et al., 1980; Maciel et al., 1985; Gildley, 1992). These have not yet been attempted on fruit samples, to our knowledge. Solids-selective NMR methods, however, would provide some advantage. Previous applications of one such method, called cross-relaxation $^1$H NMR (Wolff and Balaban, 1989; Grad and Bryant, 1990), have demonstrated its usefulness for analysis of solid phases in starch granules and gels (Wu et al., 1992; Wu and Eads, 1993), in protein (Wolff and Balaban, 1989), and in animal tisuues (Grad et al., 1991). Here we have applied this magnetization transfer technique to detect and quantify solid components and to follow their changes during ripening of banana. We have also used the liquid MAS technique to follow changes in liquid-phase composition of the same samples during ripening.

* Author to whom correspondence should be addressed [telephone (317) 494-1749; fax (317) 494-7953].

## MATERIALS AND METHODS

**Sample Preparation.** Bananas were purchased in a local supermarket at their very green stage and were ripened at room temperature (22 ± 2 °C) in normal fluorescent light for about 10 h per day. In the later text, green banana means very green at time of purchase, and ripe means fully yellow with light brown spots just appearing. Samples were taken from individual bananas from a single bunch which was very green when first obtained. Every day or every other day, a cylindrically shaped piece of edible tissue was cut from a different banana and transferred to a MAS rotor. The zirconia rotor (7-mm o.d.; 0.8-mm wall thickness; 20-mm overall length) was sealed with caps equipped with tight-fitting O-rings. Sample length is about 9 mm, and volume is 0.35 mL.

Banana tissue with water ($H_2O$) replaced by deuterium oxide ($D_2O$) was prepared for direct wide-line $^1$H NMR. Without substitution, the water proton signal interferes with detection of the solid $^1$H signal (see NMR Methods). Green banana slices about 2 cm long were weighed, freeze-dried overnight, and then weighed again. Water removed corresponded to about 72% of original weight of tissue. Banana pulp is reported to contain 70–76% moisture (Loesecke, 1950; Ockerman, 1991). Shrinkage of outer dimensions was about 10–15%. No discernible browning was observed. A cylindrical plug was cut from the freeze-dried tissue and placed in the MAS rotor. A volume of $D_2O$, equivalent to the volume of $H_2O$ removed, was added and allowed to equilibrate for several hours before measurement by wide-line Fourier transform $^1$H NMR. $D_2O$ is apparently absorbed well by the freeze-dried banana tissue, since no liquid could be poured off after equilibration.

Dry banana starch in granule form obtained from mature green stage banana pulp was a gift from Prof. Roy Whistler. This starch contained 7% water. Banana starch at 20 wt % was suspended in 0.5 wt % xanthan aqueous solution ($H_2O$).

Analytical grade sucrose, fructose, and glucose were obtained

0021-8561/93/1441-1035$04.00/0 

from Mallinckrodt Inc. (Paris, KY). Deuterium oxide (99.9 atom % D) was obtained from Aldrich (Milwaukee, WI).

**NMR Methods.** NMR spectra were acquired on a Nicolet NT 200 NMR spectrometer, with a 4.7-T superconducting solenoid magnet. The spectrometer operating frequency is 200.067 MHz for $^1$H. The spectrometer had been upgraded with a TecMag (Houston, TX) Libra interface and Macintosh IIfx data system running TecMag MacNMR data acquisition and processing software. For MAS experiments the rotor axis makes an angle of 54° 44′, the "magic angle", with the static applied field. A two-channel probe equipped for magic angle spinning (Doty Scientific, Inc., Columbia, SC) was used. For $^1$H MAS experiments, the high-frequency channel was used for both $^1$H excitation and detection. Sample temperature was maintained at 22 ± 2 °C.

For single-pulse experiments the sequence $(D_0$–$P_1$–acquisition$)_n$ was used, where $D_0$ is a delay selected to be about 15 s, which is at least 5 times longer than the longest $^1$H longitudinal relaxation time ($T_1$) in the fruits observed, $P_1$ is the radio frequency (rf) excitation pulse. The 7-μs value for $P_1$ produced a 90° tip angle in samples such as glucose in water or a standard sample (10% $D_2O$, 90% $H_2O$); however, for fresh banana tissue, the effective 90° pulse required was 14 μs, due to limited ability to tune the probe on such dielectrically lossy samples. Multiples of four scans were accumulated using quadrature phase cycling. Typical sweep width was 4 kHz, with a data size of 4096 points. Typical acquisition times were 1.02 s. Free induction decays (FIDs) were multiplied by an exponential function (line broadening of 1 Hz) to improve signal-to-noise ratio.

For water peak suppression by presaturation, the following pulse sequence was used: $(D_0$–$P_2$–$P_1$–acquisition$)_n$, where the presaturation pulse $P_2$ was applied exactly at the water resonance frequency. On the NT200, this is accomplished using the decoupler channel in heteronuclear mode. The presaturation pulse duration was 400 ms, and the presaturation rf field strength was 330 Hz (proton precession frequency).

To optimize sample condition during NMR measurements, the minimum stable spinning rate was used, as described by Ni and Eads (1992). In the spectra reported here, MAS rates were 500–1000 Hz.

Cross-relaxation NMR experiments were carried out as previously described (Grad and Bryant, 1990; Wu et al., 1992). The pulse sequence is similar to that of the water saturation experiment, except that the radiofrequency of the saturation pulse is varied from −50 to +50 kHz relative to the water resonance. The proton precession frequency in the saturation rf field was adjusted to be 1000 Hz. This value is somewhat larger than that used previously but was necessary to achieve adequate saturation of the protons in solid phases, which are at low concentration in ripe tissue. In the cross-relaxation spectrum, the ordinate is $(1 - M_A^Z/M_A^{Z0})$, i.e., the relative saturation of the water peak, and the abcissa is the offset frequency (saturation pulse radiofrequency minus water resonance frequency). Here $M_A^Z$ is water intensity with saturation pulse, and $M_A^{Z0}$ is water intensity without saturation. The cross-relaxation spectra so obtained showed broader and narrower components superimposed. These were deconvoluted into a sum of Gaussian and Lorentzian functions by the curve-fitting method of Wu and Eads (1993).

Transverse relaxation in the broader component was obtained from the saturation field strength dependence of the line width as given by (Grad and Bryant, 1990)

$$(\Delta\nu_{1/2})^2 = 2\nu_2^2 f\{(R_{BA}/R_A + 1)/R_B T_{2B}[R_{BA}/R_B + f(R_{BA}/R_A + 1)]\} + 1/\pi^2 T_{2B}^2 \quad (1)$$

where $\Delta\nu_{1/2}$ is the width (kHz) at half-height of the broader component, $\nu_2$ is the precession frequency in the saturation field, $f$ is the effective stoichiometric ratio of solid protons to liquid protons, $R_{BA}$ is the cross-relaxation rate, $R_A$ and $R_B$ are the longitudinal relaxation rates of liquid and solid, respectively, and $T_{2B}$ is the characteristic time of transverse relaxation for the solid. $T_{2B}$ is obtained from the intercept $[\Delta\nu_{1/2}(0)]$ of a plot of the square of broader component width $\Delta\nu_{1/2}$ vs the square of the offset frequency $\nu_2$ (Figure 4) as follows:

$$T_{2B} = 1/\pi\Delta\nu_{1/2}(0) \quad (2)$$

At very low precession frequencies, corresponding to very low power irradiation, the saturation was very weak, and line widths obtained by deconvolution became less certain. Thus, data obtained below $\nu_2^2 = 0.2$ kHz$^2$ were not used in the construction of Figure 4.

The wide-line and high-resolution $^1$H NMR spectrum was obtained on $D_2O$-substitued banana tissue using a solid-echo pulse sequence $(90°_x$–$\tau_1$–$90°_y$–$\tau_2$–$t)_n$ (Mansfield, 1965), where the 90° pulse width was 12 μs, $\tau_1 = 8$ μs, $\tau_2 = 6$ μs, $n = 256$. A sweep width of 1 MHz (dwell 1.0 μs) was used while the sample spun at the magic angle. Phase alternation consistent with quadrature detection was employed. The signal beginning at the top of the echo was apodized with an exponential function corresponding to 20-Hz line broadening and then Fourier transformed. Digital resolution in the spectrum was 30.5 Hz/point. $D_2O$ substitution is required since wide-line $^1$H NMR for solids detection is futile in high water content samples, such as native fruit tissues. In such samples the intensity of the wings of the water peak is comparable to the intensity of the solid resonance even at offset frequencies as large as 10–20 kHz.

**Quantitation of NMR Spectra.** Calculation of total sugars in a banana sample was made by comparison of the integral over all sugar resonances in its liquid NMR spectrum with the same integral in the spectrum of a solution of glucose plus fructose at known total concentration. The calibration spectrum was obtained under the same conditions as the experimental spectra. The result was divided by the NMR sample weight to obtain sugars as percent of fresh weight.

The relative fractions of different sugar components in banana were estimated by first measuring the standard NMR spectra on separate samples of aqueous solutions of sucrose, fructose, and glucose at known concentrations and then simulating an observed banana spectrum by adding appropriate fractions of standard spectra until the shape of the observed spectum was reproduced. This procedure, carried out by computer using standard NMR data processing software, is represented by the formula

$$I = a_s I_s + a_f I_f + a_g I_g \quad (3)$$

where $I$ is the simulated spectrum, $I_i$ are the standard spectra, and $a_i$ are the relative fractions of sugars.

## RESULTS AND DISCUSSION

**Solid Phases in Banana.** The evolution of solid-like phases in banana during ripening was monitored by the solid-selective cross-relaxation technique of $^1$H NMR of Grad and Bryant (1990), which was previously shown to be sensitive to both crystalline and noncrystalline solid-like domains in starch gels (Wu et al., 1992; Wu and Eads, 1992). The results are presented in Figure 1. It is clear that during ripening there is a dramatic decrease in area. In the first approximation, the total area of the cross-relaxation spectrum is proportional to the total solid-like mass in the sample. The observed decrease is consistent with the well-known fact that unripe banana is rich in starch and that starch is converted almost completely to soluble sugars during ripening (Loesecke, 1950; Palmer, 1971; Kays, 1991). Due to the sensitivity of the experiment to instrumental parameters, care was taken to obtain all measurements under the same conditions, including saturation radio frequency field strength.

The shapes of the cross-relaxation spectra suggest that broader and narrower components are superimposed and that the broader component decreases during ripening. This was investigated in more detail by simulating the observed spectrum as the sum of a broader Gaussian plus a narrower Lorentzian function (Wu and Eads, 1992). The results are presented in Figure 2, where it is clear that the area of the broader component decreases dramatically while its width remains fairly constant. In contrast, the area of the narrower component increases slightly during ripening while its line width also remains fairly constant.

The cross-relaxation spectrum reports the presence of molecularly rigid components. In fruit these would be

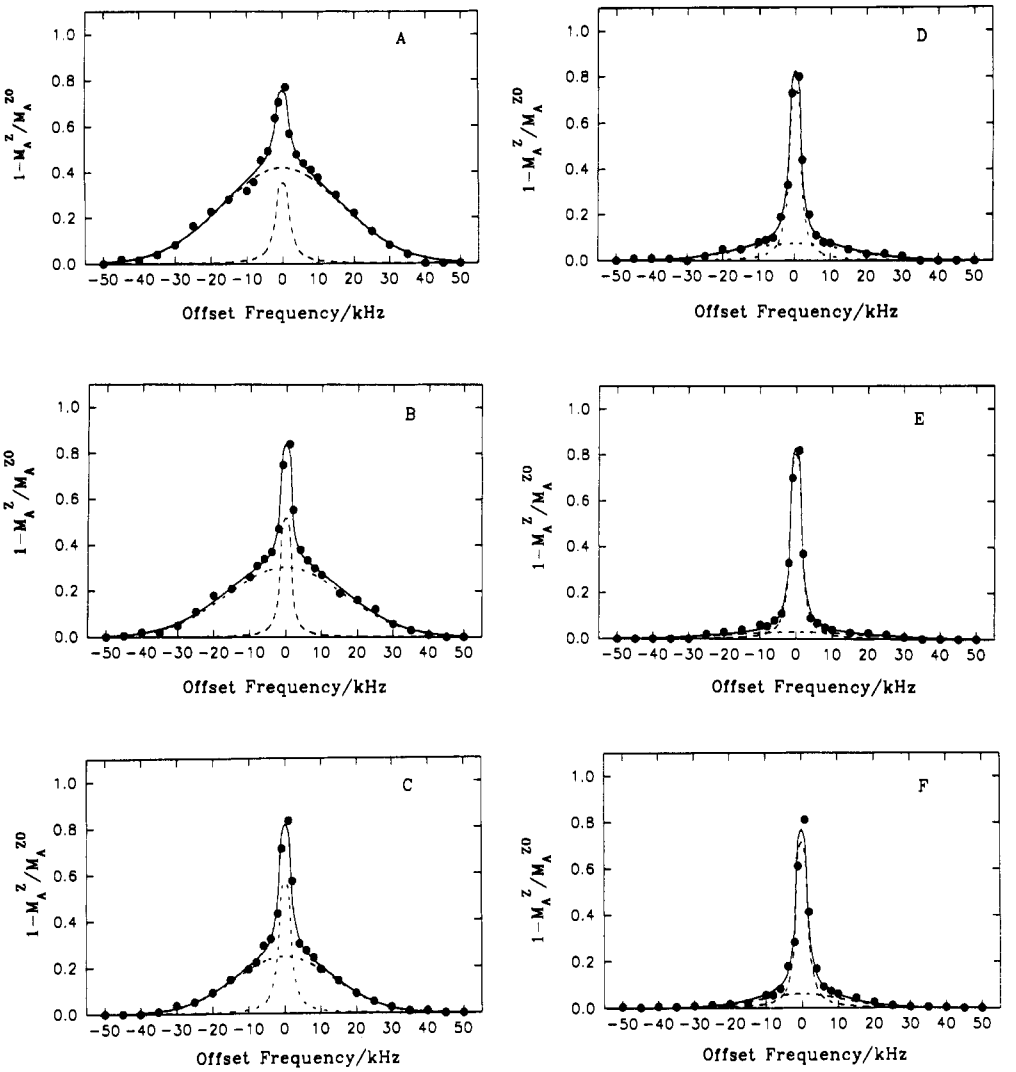


**Figure 1.** Evolution of solid-like components in banana during ripening at 20 °C: magnetization transfer spectra. Spectra were constructed as described under Materials and Methods. (●) Experimental data; (solid line) fit to sum of a narrow Lorentzian line and a broad Gaussian line (dashed lines). Measurements were taken at 1, 2, 3, 4, 6, and 8 days after purchase (spectra A, B, C, D, E, and F, respectively), on individual bananas from a single bunch. The bunch was very green on day 0.

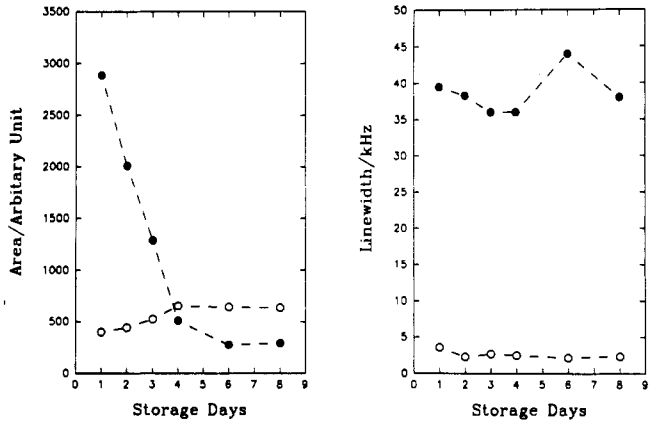


**Figure 2.** Evolution of line width and area of two solid-like components in banana during ripening. (A, left) Change in areas of broad (solid circles) and narrow (open circles) components of magnetization transfer spectra shown in Figure 1. (B, right) Change in line widths of these components. Cross-relaxation spectra were deconvoluted as described previously (Wu and Eads, 1993).

dominated by macromolecules in cell walls and organelles. The types of macromolecules and their estimated amounts in banana include starch [18% green to 1% ripe (Beaudry et al., 1989)], cellulose [2–3% green, slightly less in ripe (Loesecke, 1950)], hemicellulose [0.2% green to 0.1% ripe (Loesecke, 1950)], protopectin [0.6 green to 0.35% ripe (Loesecke, 1950)], pectin [0.2% green to 0.6% ripe (Loesecke, 1950)], and protein [1%, stage of ripeness not specified (Ockerman, 1991)]. It is well-known that cellulose, starch, and a certain fraction of pectins are very rigid, i.e., producing $^1$H NMR line widths of the order of tens of kilohertz (Mackay et al., 1982). Thus, the broad component in banana cross-relaxtion spectra probably includes these compononts. It is also known that pectins can produce a signal of intermediate mobility, of width of the order of 3 kHz. Thus, the narrower component in banana cross-relaxation spectra probably contains this component. The mobilities of the other macromolecular compononts mentioned have not been investigated very thoroughly. Thus, it is not possible at this time to assign them to either the broad or the narrow cross-relaxation components.

Attempts to obtain a direct measurement of the full $^1$H NMR spectrum by single-pulse or solid-echo $^1$H NMR were not successful, since the liquid-phase components, primarily water, produce intensities comparable to or exceeding solid intensity even at frequencies as far as tens of kilohertz from the water resonance. To reduce water proton intensity, water ($H_2O$) was removed by freeze-drying and replaced with deuterium oxide ($D_2O$) as

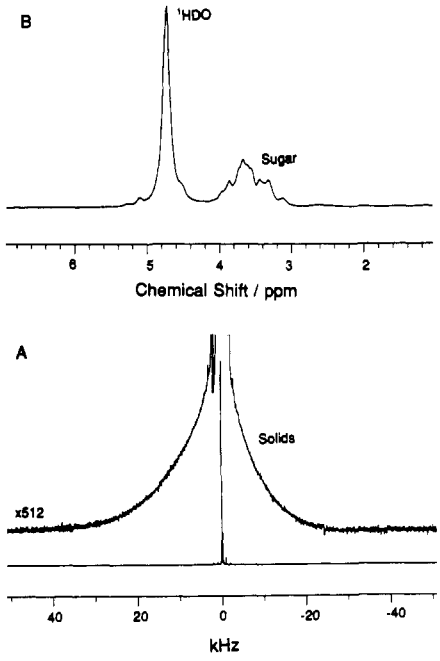


**Figure 3.** Wide-line and high-resolution 200-MHz $^1$H NMR spectrum of banana with water ($H_2O$) replaced by deuterium oxide ($D_2O$). The spectrum was obtained by the solid-echo method while the sample was spinning at the magic angle at 1000 Hz. (A) The full width display, no vertical expansion, only sharp resonances corresponding to the $^1$HDO peak, its spinning side bands, and sugars are evident. With vertical expansion (×512), the broad components are evident, the broadest component corresponding to starch and rigid cell wall components. (B) Horizontal expansion of the central 1.2% of the lower spectrum in (A). Note change to chemical shift scale ($^1$HDO peak assigned to 4.76 ppm as internal reference). Resonances are assigned in Figure 6.

described under Materials and Methods. The wide-line spectrum obtained with the solid-echo pulse sequence and magic angle spinning is displayed in Figure 3. It is clear from the vertical expansion (Figure 3A) that a very broad resonance, of width approximately 25 kHz, is present and that a narrower resonance, of width approximately 3 kHz, may also be present, although it is difficult to distinguish this from the wings of the combined sugar and residual $^1$HDO peaks. The broader resonance comes from rigid domains, and its width in this case is consistent with that of hydrated starch granules (Wu et al., 1992). A somewhat broader contribution is expected from the cellulosic solids in cell walls (MacKay et al., 1982). However, estimates of cellulose content in banana range from 1 to 2 wt %, while starch ranges from 18 (unripe) to about 1 wt % (ripe). Thus, starch is expected to dominate the broad component in the wide-line $^1$H NMR spectrum. The result in Figure 3A supports the premise that the cross-relaxation spectrum should correspond closely to the true wide-line spectrum and also supports the idea that starch dominates the broader component in the cross-relaxation spectra in Figure 1. The horizontally expanded central portion of the $^1$H NMR spectrum of $D_2O$-substituted banana (Figure 3B) shows liquid-phase resonances with resolution comparable to that in a conventional high-resolution spectrum. The appearance of sugar resonances with narrow, liquid-like line widths is consistent with the obvious expectation that sugars return to a dissolved state after the process of freeze-drying and rehydration with $D_2O$ (Figure 3B).

Cross-relaxation line width is dependent on the $T_2$ of solid-phase protons which, in turn, is sensitive to internal molecular motions. However, the line width is also affected by nuclear relaxation processes other than those associated

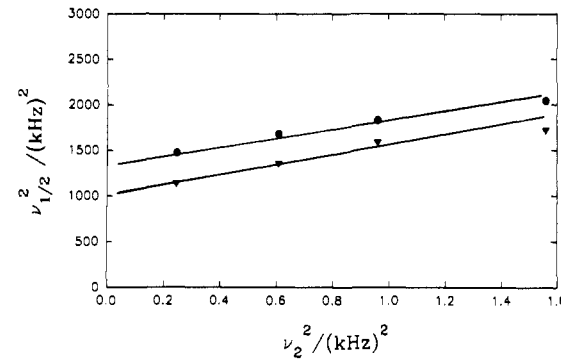


**Figure 4.** Determination of transverse relaxation time of banana starch. The line width $\Delta\nu_{1/2}$ was measured as a function of precession frequency $\nu_2$ in the $^1$H saturation field in a cross-relaxation experiment, and the squares of these quantities were plotted as shown. Transverse relaxation time $T_{2B}$ was determined from the intercept as described under Materials and Methods. $T_{2B}$ for the starch in green banana (▼) was found to be 9.9 μs; $T_{2B}$ for a suspension of banana starch (●) was found to be 8.8 μs.

with the solid-phase protons, making it risky to interpret line width purely in terms of rigidity. The line width in the wide-line spectrum would be more reliable, but the superimposed broad components have not yet been analyzed in a physically legitimate way (Lacelle and Gerstein, 1987). Thus, a more direct measurement of transverse relaxation time $T_{2B}$ of solid-phase protons was undertaken. The intercept method of Grad and Bryant (see Materials and Methods) was applied to two samples: intact green banana tissue and an aqueous suspension of banana starch granules isolated from green banana. The result is shown in Figure 4. The observed $T_2$ values are almost identical, and the value near 10 μs is characteristic of rigid crystalline solids, giving further support to the proposal that the broad component in cross-relaxation and wide-line spectra is dominated by starch in hydrated granule form. This method was also applied to the cross-relaxation data for hydrated cornstarch given in Swanson's paper (Swanson, 1991), yielding a $T_2$ value of 11 μs for the cornstarch. This value is close to our results of 9.9 and 8.8 μs for green banana and banana starch suspension, respectively. Taken together, these results show that transverse relaxation times of protons in hydrated starch granules from different sources fall in the same range.

**Liquid Phases in Banana.** The well-known increase in soluble carbohydrate during ripening is easily monitored by high-resolution $^1$H NMR, using the combination of MAS to reduce broadening due to susceptibility inhomogeneity (Doskocilova et al., 1975; Ni and Eads, 1992) and water peak suppression to permit detection of all non-water components with full sensitivity (Ni and Eads, 1993). The well-resolved resonances of sugars are shown in the series of spectra of Figure 5. Assignments are given in Figure 6. It is important to note that these spectra were obtained on the same samples represented by the cross-relaxation spectra in Figure 1. The increase in sugar resonance intensity is obvious and can be quantified by integration, as shown below. However, close inspection of the spectra in Figure 5 also reveals changes in sugar composition during ripening. Thus, an attempt was made to simulate each of these spectra using a set of standard spectra obtained on aqueous solutions of pure sucrose, fructose, and glucose at known concentrations. The results were expressed in the familiar units of percent of fresh weight and also in terms of milliequivalents of component hexoses, to facilitate comparison among hexose carbohydrates of different degrees of polymerization. Very green and very ripe samples are compared (Table I). The dramatic change in

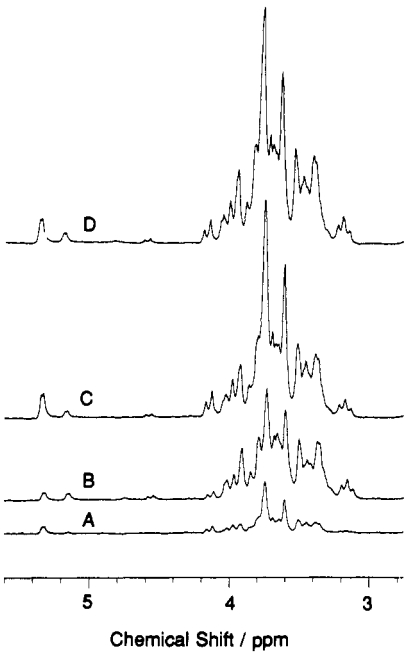


**Figure 5.** Evolution in soluble sugars during banana ripening detected by $^1H$ MAS NMR with water peak suppression. Data were obtained on the same samples used for magnetization transfer experiments (Figure 1). Spectra A, B, C, and D were measured at 1, 2, 3, and 6 days of storage, respectively (for clarity, days 4 and 8 are not shown). Only the carbohydrate region is shown. Sixteen scans were taken for each spectrum.

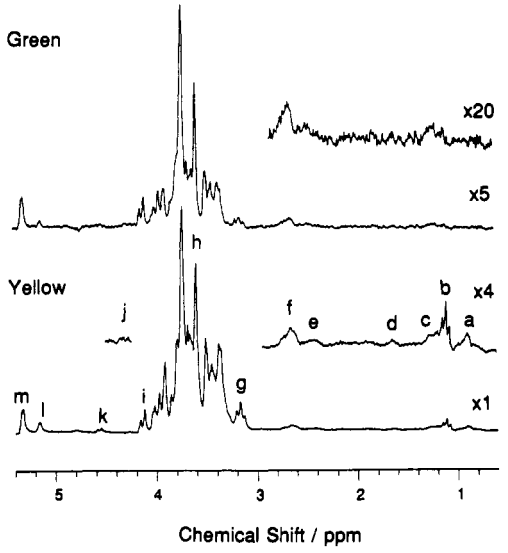


**Figure 6.** Comparison between green (same spectrum as in Figure 5A) and ripe banana (same as Figure 5B) with liquid-phase resonances detected by $^1H$ MAS NMR with water peak suppression. Vertical scaling was adjusted to facilitate comparison. Assignments are as follows: (a) methyl group ($CH_3$) of fatty acids (palmitic, linoleic, and linolenic acids); (b) unassigned; (c–e) methylene group ($CH_2$) of fatty acids; (f) $CH_2$ group of malic or citric acid and possibly overlapping lipid methylene; (g) $\beta$-Glu H-2; (h) mixed Glu, Fru, and Suc ring protons; (i) Suc H-3′; (j) CH group of malic acid; (k) $\beta$-Glu H-1; (l) $\alpha$-Glu H-1; (m) Suc H-1 and CH=CH in unsaturated acids.

the amount of each component is evident. In addition, the ratio of sucrose/fructose/glucose changes from 75:11:14 (as weight percent of total sugar) for green banana to 47:24:29 for ripe banana, in close agreement with several previous studies (Ensminger et al., 1983; Ockerman 1991; Beaudry, 1989). The NMR method for estimation of sugar composition is direct and apparently accurate, while the limits of precision have yet to be established. Quantitative

**Table I. Concentrations of Sucrose, Glucose, and Fructose in Pulp of Green and Ripe Banana**

| | concentration[a] | | | |
|---|---|---|---|---|
| | mmol of hexose/g | | % of fresh wt | |
| component | green | ripe | green | ripe |
| sucrose | 1.30 | 5.0 | 2.2 | 8.5 |
| glucose | 0.21 | 2.4 | 0.4 | 4.3 |
| fructose | 0.26 | 3.0 | 0.5 | 5.3 |
| total sugar | 1.77 | 10.4 | 3.1 | 18.1 |

[a] Determined by low-speed magic angle spinning $^1H$ NMR as described in the text.

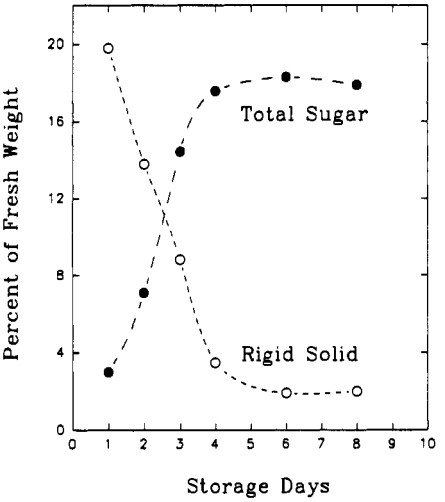


**Figure 7.** Hydrolytic conversion of starch to sugars during banana ripening detected by NMR. (●) Total sugar; (○) starch. Methods of calculation of starch and total sugar contents are given in the text.

NMR could be used to resolve such questions as whether fructose and glucose are the hydrolytic products of sucrose during banana ripening (Beaudry, 1989). It is conceivable to use extensions of these methods (e.g., two- or three-dimensional MAS NMR) to detect carbohydrate metabolites and intermediates present at much lower concentrations.

The level of compositional detail that can be obtained with this method is further illustrated in Figure 6, which compares green with ripe (same as spectra in Figure 5A,D). In addition to the changes in sugar composition, changes in lipid and organic acid components are also evident. These components could be quantified by combination of calibration and spectral simulation methods. If any fraction of lipid or organic acid were in a solid phase, it would not be detected in these experiments.

**Conversion of Starch to Sugars.** Total rigid solid and total sugars as percent of fresh weight were obtained from calibration of cross-relaxation and high-resolution spectra, respectively, and plotted vs storage days in Figure 7. The overall decrease in rigid component in cross-relaxation spectra is from 20 to 2 wt %, while total sugar changes from 3.0 to 18.3 wt %, with a slight decrease from this value as the fruit becomes overripe. The shape of this graph is very similar to that obtained previously (Beaudry, 1989) using careful chemical analysis. In that paper, actual starch was measured by grinding the sample, extracting soluble sugars, gelatinizing the starch, hydrolyzing with amyloglucosidase, derivatizing the sugars, and gas chromatography. Their method for sugars similarly required grinding, extraction, derivatization, and chromatography. On the other hand, we measured both sugars and rigid component spectroscopically, with no physical

disruption of the tissue other than cutting a sample plug and without use of chemical reagents, chromatography, or of spectrometry other than NMR.

**Conclusions.** In a separate paper we have described a nondestructive chemical analysis of liquid-phase components in fruits by proton magic angle spinning NMR (Ni and Eads, 1993). The work described here supplements the chemical analysis with information about solid phases obtained simultaneously on the same samples. To our knowledge, this is the first report on analyses of both solid and liquid components in samples of intact fruit tissue using a nondestructive method. The usefulness of obtaining both kinds of information is clearly demonstrated in Figure 6, which associates disappearance of starch with accumulation of soluble sugars during ripening in banana. This result is wholly consistent with the model that the rate of sugar accumulation represents gluconeogenic carbon flux (Beaudry et al., 1989). In principle, each sample could be subjected to further analysis by performing NMR experiments sensitive to other chemical and physical quantities.

While the results reported here were obtained on a research grade spectrometer, the cross-relaxation experiment can, in principle, be executed on a low-field (5–20 MHz), low-resolution, single-frequency ($^1$H) spectrometer of low relative cost. Additionally, both the cross-relaxation and the high-resolution experiments can, in principle, be executed on a lower field (60–100 MHz), high-resolution, single-frequency spectrometer with magic angle spinning accessory, also far less costly than research grade NMR equipment. This suggests that the methods described can be used for quality assessment, process control, and proximate analysis.

## ACKNOWLEDGMENT

This is Paper 13697 of the Agricultural Experiment Station, Purdue University, West Lafayette, IN. We gratefully acknowledge financial assistance from the sustaining members of the Whistler Center for Carbohydrate Research, Purdue University. We thank Drs. Qing-Wen Ni and Perry Pellechia for helpful suggestions.

## LITERATURE CITED

Baianu, I. C.; Förster, H. Cross-Polarization, High-Field Carbon-13 NMR Techniques for Studying Physicochemical Properties of Wheat Grain, Flour, Starch Gluten and Wheat Protein Powders. *J. Appl. Biochem.* **1980**, *2*, 347–354.

Beaudry, R. M.; Severson, R. F.; Black, C. C.; Kays, S. J. Banana Ripening: Implications of Changes in Glycolytic Intermediate Concentration, Glycolytic and Gluconeogenic Carbon Flux, and Fructose 2,6-Bisphosphate Concentration. *Plant Physiol.* **1989**, *91* (1), 436–444.

Bellon, V.; Cho, S. I.; Krutz, G. W.; Davenel, A. Ripeness Sensor Development based on Nuclear Magnetic Resonance. *Food Control* **1992**, Jan, 45–48.

Chen, P.; McCarthy, M. J.; Kauten, R. NMR for Internal Quality Evalution of Fruits and Vegetables. *Am. Soc. Agric. Eng.* **1989**, *32*, 1747–1753.

Cho, S. I.; Bellon, V.; Eads, T. M.; Stroshine, R. L.; Krutz, G. W. Sugar Content Measurement in Fruit Tissue Using Water Peak Suppression in High Resolution $^1$H Magnetic Resonance. *J. Food Sci.* **1991**, *56*, 1091–1094.

Coombe, B. G.; Jones, G. P. Measurement of the Changes in the Composition of Developing Undetached Grape Berries by Using $^{13}$C NMR Techniques. *Phytochemistry* **1983**, *22*, 2185–2187.

Doskocilova, D.; Tao, D. D.; Schneider, B. Effect of Macroscopic Spinning Upon Linewidth of NMR Signals of Liquid in Magnetically Inhomogeneous Sysyems. *Czech. J. Phys.* **1975**, *B25*, 202–209.

Eads, T. M. Multinuclear High Resolution and Wide Line NMR Method for Analysis of Lipids. In *Analysis of Fats, Oils, and Lipoproteins*; Perkins, E. G., Ed.; American Oil Chemists' Society: Champaign, IL, 1991; pp 409–457.

Ensminger, A. N.; Ensminger, M. E.; Konlande, J. E.; Robson, J. R. K. *Food & Nutrition Encyclopedia*; Pegus Press: Clovis, CA, 1983; Vol. 1, p 341.

Gildley, M. J. High Resolution Solid State NMR of Food Materials. *Trends Food Sci. Technol.* **1992**, *3*, 231–236.

Grad, J.; Bryant, R. G. Nuclear Magnetic Cross-Relaxation Spectroscopy. *J. Magn. Reson.* **1990**, *90*, 1–8.

Grad, J.; Mendelson, D.; Hyder, F.; Bryant, R. G. Application of Nuclear Magnetic Cross-Relaxation Spectroscopy to Tissues. *Magn. Reson. Med.* **1991**, *17*, 452–459.

Ishida, N.; Kobayashi, T.; Koizumi, M.; Kano, H $^1$H-NMR Imaging of Tomato Fruits. *Agric. Biol. Chem.* **1989**, *53*, 2363–2367.

Kays, S. J. *Postharvest Physiology of Perishable Plant Products*; Van Nostrand Reinhold: New York, 1991; p 274.

Lacelle, S.; Gerstein, B. C. NMR Studies on the Presence of Domain Structures in Polysaccharides. *Biopolymers* **1987**, *26*, 849–861.

Loesecke, H. W. V. *Bananas*; Interscience Publishers: London, 1950; Chapter 4.

Maciel, G. E.; Haw, J. F.; Smith, D. H.; Gabreilsen, B. C.; Hatfield, G. R. Cabon-13 Nuclear Magnetic Resonance of Herbaceous Plants and Their Components, Using Cross Polarization and Magic-Angle Spinning. *J. Agric. Food Chem.* **1985**, *33*, 185–191.

MacKay, A. L.; Bloom, M.; Taylor, I. E. P. Broadline Proton Magnetic Resonance Study of Cellulose, Pectin, and Bean Cell Walls. *Biopolymers* **1982**, *21*, 1521–1534.

Mansfield, P. Multiple-Pulse Nuclear Magnetic Resonance Transients in Solids. *Phys. Rev.* **1965**, *137*, A961–A974.

Ni, Q. W.; Eads, T. M. Low-speed Magic-Angle-Spinning Carbon-13 NMR of Fruit Tissue. *J. Agric. Food Chem.* **1992**, *40*, 1507–1513.

Ni, Q. W.; Eads, T. M. Liquid-Phase Composition of Intact Fruit Tissue Measured by High-Resolution Proton NMR. *J. Agric. Food Chem.* **1993**, preceding paper in this issue.

Ockerman, H. W. O. *Food Science Sourcebook, Part 2, Food Composition Properties, and General Data*; Van Nostrand Reinhold: New York, 1991; p 861.

Palmer, J. K. The Banana. In *The Biochemistry of Fruits and Their Products;* Halme, A. C., Ed.; Academic Press: London, 1971; Vol. 2, pp 65–103.

Swanson, S. D. Broadband Excitation and Detection of Cross-Relaxation NMR Spectra. *J. Magn. Reson.* **1991**, *95*, 615–618.

Wang, S. W.; Wang, P. C. Non-Destructive Detection of Watercore in Apple with Nuclear Magnetic Resonance Imaging. *Sci. Hortic. (Amsterdam)* **1988**, *35*, 227–234.

Wang, S. W.; Wang, P. C. Non-Destructive Detection of Core Breakdown in Bartlett Pears with Nuclear Magnetic Resonance Imaging. *HortScience* **1989**, *24*, 106–190.

Wolff, S. D.; Balaban, R. S. Magnetization Transfer Contrast (MTC) and Tissue Water Proton Relaxation in Vivo. *Magn. Reson. Med.* **1989**, *10*, 135–144.

Wu, J. Y.; Eads, T. M. Evolution of Polymer Mobility During Ageing of Gelatinized Waxy Maize Starch: A Magnetization Transfer $^1$H NMR Study. *Biopolymers* **1993**, *20*, 51–60.

Wu, J. Y.; Bryant, R. G.; Eads, T. M. Detection of Solid-like Components in Starch Using Cross-Relaxation and Fourier Transform Wide-Line $^1$H NMR Methods. *J. Agric. Food Chem.* **1992**, *40*, 449–455.

Received for review January 22, 1993. Accepted April 20, 1993.